16th World Conference on Earthquake, 16WCEE 2017

Santiago Chile, January 9th to 13th 2017

Paper N° 594

Registration Code: S-Z1462378856

BEHAVIOR OF INVERTED PENDULUM CYLINDRICAL STRUCTURES THAT ROCK AND WOBBLE DURING EARTHQUAKES

S. Burger (1), M. Egger(2), J. A. Bachmann (3), M. F. Vassiliou(4), B. Stojadinovic (5)

(1) *M.Sc. Student, Chair of Structural Dynamics and Earthquake Engineering, IBK, ETH Zürich, burgerst@student.ethz.ch*
(2) *M.Sc. Student, Chair of Structural Dynamics and Earthquake Engineering, IBK, ETH Zürich, megger@student.ethz.ch*
(3) *PhD Candidate, Chair of Structural Dynamics and Earthquake Engineering, IBK, ETH Zürich, bachmann@ibk.baug.ethz.ch*
(4) *Senior Researcher, Chair of Structural Dynamics and Earthquake Engineering, IBK, ETH Zürich, vassiliou@ibk.baug.ethz.ch*
(5) *Professor, Chair of Structural Dynamics and Earthquake Engineering, IBK, ETH Zürich, stojadinovic@ibk.baug.ethz.ch*

Abstract

The in-plane (2d) response of rigid rocking blocks has been extensively studied. In order to use rocking as a seismic response modification strategy for large structures (such as bridges and chimneys), the rocking motion of bodies in two orthogonal planes (3d rocking) needs to be explored first. Dynamic models of systems allowed to step out or roll out of their initial position and rocking plane have received attention. However, under earthquake excitation such systems may remain stable, but often end their motion with significant residual displacements with respect to their starting position. Such behavior is not acceptable for real structures. This paper studies the 3d motion of a rigid cylinder that is allowed to uplift and sustain rocking and wobbling motion without sliding or rolling-out of its initial position. Like a rectangular body in 2d rocking motion, the cylinder has zero residual displacement at the end of its 3d motion. The 3d dynamic model of the cylinder has two degrees of freedom, making it the simplest 3d extension of Housner's classical rocking model. The development of the 3d cylinder model is presented first. This model is computationally inexpensive and simple enough to perform extensive parametric analyses to understand the roles of the dominant parameters of the 3d rocking and wobbling (unsteady rolling) motion. Modes of motion of the cylinder are identified and presented. Finally, 3d rocking and wobbling spectra are constructed and compared with the classical 2d rocking spectra, to indicate that, in many cases, the 2d approach may lead to unconservative estimates of 3d rocking and wobbling response.

Keywords: rocking isolation; 3d rocking motion; uplifting structures;

1. Introduction

To the authors' knowledge, the first modern interest in rocking structures stemmed from the need to estimate the peak acceleration of ground motions by studying overturned blocks. In 1885, Milne [1] published a study which hinges upon the assumption that the uplifting acceleration of a rigid block is enough to overturn it. In an effort to construct an acceleration measuring device, in 1927 Kirkpatrick [2] uncovered that the overturning of a block does not only depend on the ground motion PGA and on the block slenderness, but on but on the ground motion duration and the block size. In 1963, Housner [3] published his seminal paper where he explained the remarkable properties of rocking structures: (a) the larger of two geometrically similar blocks can survive the excitation that will topple the smaller block, and (b) of two same-acceleration amplitude pulses, the one with longer duration is more capable of inducing overturning. These properties, as well as the observation that modern and ancient structures that were unintentionally designed to rock behaved well during earthquakes, have motivated engineers to try to use uplifting of structures as a seismic modification technique. Since then numerous papers have been published, both on solitary blocks [4-33] and on assemblies of rocking bodies [34-42].

All of the above papers treat rocking as a 2d, in-plane problem. The published work on the dynamic response of 3d rocking of rigid bodies is much more limited. In [43-45] the motion of a rigid cylinder under seismic excitation is studied. Other researchers studied the 3d response of ancient conical or cylindrical columns numerically [46, 47], or experimentally [48-50]. Makris et al. [51] experimentally tested scaled models of uplifting bridges [51]. All the above studies conclude that 3d motion is present (so called "wobbling"), even under 2d initial conditions or under single-horizontal-component ground excitation. In fact, Stefanou et al. [52] proved the above observation theoretically. When the initial spin tends to zero, the rocking and wobbling of a rigid cylinder involves a sudden rapid motion of the contact point around the circular base. Srinivasian and Ruina [53] proved that, surprisingly, the net angle of motion of this contact point is nearly independent of initial conditions. This angle of turn depends simply on the geometry and mass distribution of the body.

Beyond the scopes of earthquake engineering, Moffat [54] described the motion of a toy, the so-called "Euler's Disk" (which is not related to Euler but is named after the Euler Angles used to describe its motion). The toy comprises a disk that is given an initial spin on a chromed concave base. The toy spins with an increasing frequency and stops in an abrupt manner. Similar behavior is observed when spinning a coin. Even though there is no evident engineering application of the toy, Moffat's paper received a lot of attention and created a debate about its energy dissipation mechanisms [55-58].

The 3d behavior of non-cylindrical bodies has also recently received attention. Konstantinidis and Makris [59] and Zulli et al. [60] studied the rocking motion of a 3d prism. Chatzis and Smyth [61] studied the motion of a 3d prism on a deformable base, taking sliding into account as well as the 3d dynamics of a rigid body with wheels on a moving base [62]. Greenbaum [63] developed an interesting computer vision method that allows for the experimental measurement of the rigid body translation and rotation time histories in three dimensions.

All the above 3d models are multi degree of freedom (MDOF) and are useful for unconstrained 3d objects. On the contrary, this paper studies a simpler model: a cylinder rocking and wobbling (unsteady rolling) exclusively above the initial position of its base, without sliding. No "rolling-out" is allowed. In that sense, it is a direct extension of Housner's model, which constrains the body to restore to its original position. This 3d model is employed because, if rocking is to be used for seismic isolation, no residual deformation (not to mention roll-out motion) is desired. To achieve this, for example, a recess around a column could be used to constrain roll-out motion. The model investigated herein is much simpler and computationally cheaper than the MDOF models, thereby allowing for extensive parametric studies, which are a subject of ongoing research.

2. Model Description and Equations of Motion

2.1 Frames of Reference

The model is shown in Fig. 1. It is a rigid cylinder of mass m, base radius b and height $2h$. Its semidiagonal is denoted R and its slenderness α ($\tan\alpha = b/h$). The main assumptions of the model are:

a) The cylinder is considered rigid and homogeneous.
b) The supporting plane surface is considered rigid and therefore the contact is pointwise.
c) No damping mechanism is included.
d) The cylinder is constrained not to roll-out of its initial position.

Given the above constraints, the model has only two degrees of freedom: The tilt angle, θ, and the rolling angle, φ. The latter determines the contact point between the cylinder and the supporting plane.

The following frames of reference are used: XYZ is the inertial reference frame; xyz is pinned to the center of the bottom of the cylinder, B, and has the same orientation as XYZ; $x_3y_3z_3$ is fixed to B and follows the rotations of the cylinder. At rest all three systems have the same orientation and the last two coincide.

XYZ and xyz differ only by a translation. $x_3y_3z_3$ is a rotation of xyz. The so called 3-2-3 Euler angles are used to describe this rotation [64]. The first angle φ describes a rotation around the axis z. This leads to a new coordinate system $x_1y_1z_1$. The second angle, θ, describes a rotation around the axis y_1. This leads to the new coordinate system $x_2y_2z_2$. θ is the tilt angle. The third angle, ψ, describes a rotation around the axis y_2. This leads to the new coordinate system $x_3y_3z_3$. Since it is assumed that the friction between the cylinder and the foundation is large, it can be proven that $\psi = -\varphi$.

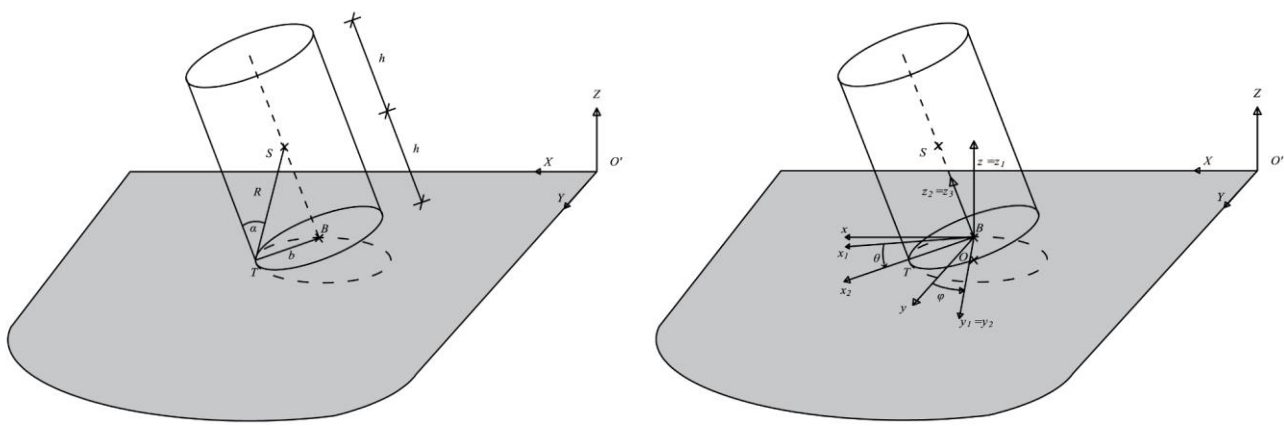

Fig.1 *Left*: Geometry of the model. The cylinder is allowed to uplift and wobble but constrained not to roll-out of its original base. *Right*: Fig. 3. "3-2-3" Euler Angles.

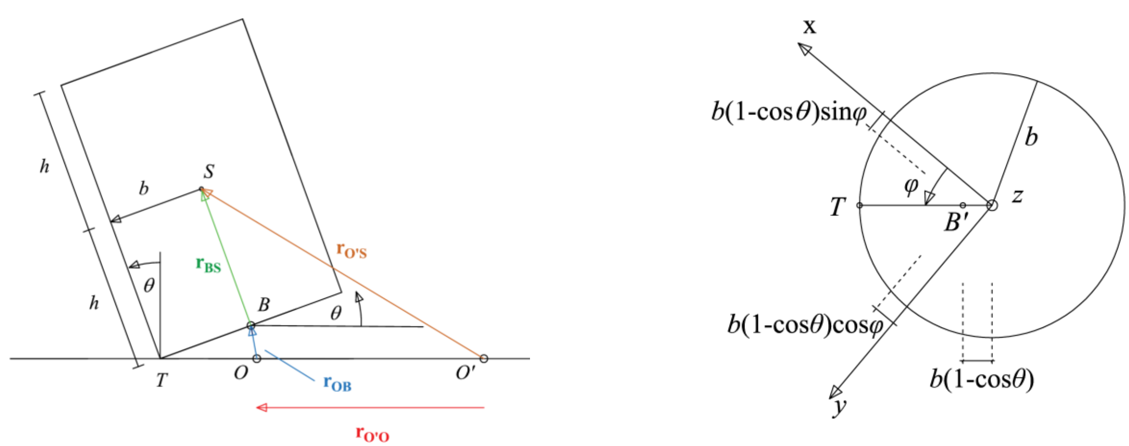

Fig.2 *Left*: Vertical section passing from the center of mass of the cylinder, S, and from the contact point with the ground, i.e. the pivot point, T; *Right*: Top View. The circle is the original configuration of the cylinder and B' is the vertical projection of B on the ground.

In order to derive the equation of motion, the translational and rotational motion of the center of mass of the cylinder should be tracked, relative to the inertial reference frame *XYZ*. Referring to Fig. 2, the position vector of the center of mass, *S*, is:

$$\mathbf{r}_{\mathbf{O'S}} = \mathbf{r}_{\mathbf{O'O}} + \mathbf{r}_{\mathbf{OB}} + \mathbf{r}_{\mathbf{BS}} \tag{1}$$

The above components can be written as:

$$\mathbf{r}_{\mathbf{O'O}} = u_{gx}\mathbf{i}_{\mathbf{X}} + u_{gx}\mathbf{i}_{\mathbf{Y}} + 0\mathbf{i}_{\mathbf{Z}} \tag{2}$$

$$\mathbf{r}_{\mathbf{OB}} = d_x\mathbf{i}_{\mathbf{x}} + d_y\mathbf{i}_{\mathbf{y}} + d_z\mathbf{i}_{\mathbf{z}} \tag{3}$$

$$\mathbf{r}_{\mathbf{BS}} = 0\mathbf{i}_{\mathbf{x}_3} + 0\mathbf{i}_{y_3} + h\mathbf{i}_{z_3} \tag{4}$$

Where **i** are the unit vectors of each frame of reference. The unit vectors are related through the following transformations:

$$\begin{bmatrix}\mathbf{i}_{\mathbf{X}}\\ \mathbf{i}_{\mathbf{Y}}\\ \mathbf{i}_{\mathbf{Z}}\end{bmatrix} = \mathbf{I}\cdot\begin{bmatrix}\mathbf{i}_{\mathbf{x}}\\ \mathbf{i}_{\mathbf{y}}\\ \mathbf{i}_{\mathbf{z}}\end{bmatrix} \quad \text{and} \quad \begin{bmatrix}\mathbf{i}_{\mathbf{x}}\\ \mathbf{i}_{\mathbf{y}}\\ \mathbf{i}_{\mathbf{z}}\end{bmatrix} = \mathbf{A}_1\cdot\mathbf{A}_2\cdot\mathbf{A}_3\cdot\begin{bmatrix}\mathbf{i}_{\mathbf{x}_3}\\ \mathbf{i}_{\mathbf{y}_3}\\ \mathbf{i}_{\mathbf{z}_3}\end{bmatrix} \tag{5}$$

where **I** is the unit matrix and $\mathbf{A}_1$ $\mathbf{A}_2$ and $\mathbf{A}_3$ are the rotation matrices that correspond to the Euler angles:

$$\mathbf{A}_1 = \begin{bmatrix}\cos\varphi & -\sin\varphi & 0\\ \sin\varphi & \cos\varphi & 0\\ 0 & 0 & 1\end{bmatrix} \quad \mathbf{A}_2 = \begin{bmatrix}\cos\theta & 0 & \sin\theta\\ 0 & 1 & 0\\ -\sin\theta & 0 & \cos\theta\end{bmatrix} \quad \mathbf{A}_3 = \begin{bmatrix}\cos\varphi & \sin\varphi & 0\\ -\sin\varphi & \cos\varphi & 0\\ 0 & 0 & 1\end{bmatrix} \tag{6}$$

With reference to Eq. (5)-(6) $\mathbf{r}_{\mathbf{BS}}$ can be written in *XYZ* coordinates:

$$\mathbf{r}_{\mathbf{BS}} = h\cdot\cos\varphi\cdot\sin\theta\cdot\mathbf{i}_{\mathbf{X}} + h\cdot\sin\varphi\cdot\sin\theta\cdot\mathbf{i}_{\mathbf{Y}} + h\cdot\cos\theta\cdot\mathbf{i}_{\mathbf{Z}} \tag{7}$$

or, as a vector

$$\mathbf{r}_{\mathbf{BS}} = h\begin{bmatrix}\cos\varphi\cdot\sin\theta\\ \sin\varphi\cdot\sin\theta\\ \cos\theta\end{bmatrix}_{XYZ} \tag{8}$$

With reference to Fig. 2 d_x, d_y and d_z from Eq. (3) are:

$$\begin{aligned} d_x &= b\cdot(1-\cos\theta)\cdot\cos\varphi\\ d_y &= b\cdot(1-\cos\theta)\cdot\sin\varphi\\ d_z &= b\cdot\sin\theta \end{aligned} \tag{9}$$

or, as a vector

$$\mathbf{r}_{\mathbf{OB}} = b\cdot\begin{bmatrix}(1-\cos\theta)\cdot\cos\varphi\\ (1-\cos\theta)\cdot\sin\varphi\\ \sin\theta\end{bmatrix}_{XYZ} \tag{10}$$

Therefore Eq. (1) can be written in *XYZ* coordinates:

$$\mathbf{r}_{\mathbf{O'S}}=\begin{bmatrix}u_{gx}\\u_{gy}\\0\end{bmatrix}_{XYZ}+b\cdot\begin{bmatrix}(1-\cos\theta)\cdot\cos\varphi\\(1-\cos\theta)\cdot\sin\varphi\\\sin\theta\end{bmatrix}_{XYZ}+h\begin{bmatrix}\cos\varphi\cdot\sin\theta\\\sin\varphi\cdot\sin\theta\\\cos\theta\end{bmatrix}_{XYZ}\tag{11}$$

2.2 Equations of Motion

The Lagrangian equations of the system are:

$$\frac{d}{dt}\left(\frac{\partial(T-V)}{\partial\dot{q}_i}\right)-\frac{\partial(T-V)}{\partial q_i}=0\tag{12}$$

where q_i are the two degrees of freedom of the system (θ and φ) while T and V are the kinetic and the potential energy of the system, respectively.

The translational kinetic energy of the system is

$$T_{trans}=\frac{1}{2}m\cdot\dot{\mathbf{r}}^T_{\mathbf{O'S}}\cdot\dot{\mathbf{r}}_{\mathbf{O'S}}\tag{13}$$

The angular velocity of the cylinder, in the $x_3y_3z_3$ coordinates is [64]:

$$\boldsymbol{\omega}=\begin{bmatrix}-\dot{\varphi}\cdot\cos\varphi\sin\theta-\dot{\theta}\cdot\sin\varphi\\-\dot{\varphi}\cdot\sin\varphi\sin\theta+\dot{\theta}\cdot\cos\varphi\\\dot{\varphi}\cdot\cos\theta-\dot{\varphi}\end{bmatrix}_{x_3y_3z_3}\tag{14}$$

The rotational kinetic energy of the system is

$$T_{rot}=\frac{1}{2}\boldsymbol{\omega}^T\cdot\mathbf{I_0}\cdot\boldsymbol{\omega}\tag{15}$$

where $\mathbf{I_0}$ is the moment of inertia tensor of the cylinder around its principal axis:

$$\mathbf{I_0}=\begin{bmatrix}I_x&0&0\\0&I_y&0\\0&0&I_z\end{bmatrix}=\begin{bmatrix}\frac{3mb^2+4mh^2}{12}&0&0\\0&\frac{3mb^2+4mh^2}{12}&0\\0&0&\frac{mb^2}{2}\end{bmatrix}\tag{16}$$

The potential energy V of the system is

$$V=mg(b\sin\theta+h\cos\theta)\tag{17}$$

Eq. (10)-(17) give the equations of motion:

$$\begin{aligned}&\left(I_1+h^2m+b^2m\right)\cdot\ddot{\theta}+bgm\cdot\cos\theta-hgm\cdot\sin\theta\\&+\left(\left(I_2-I_1+b^2m-h^2m\right)\cdot\cos\theta\cdot\sin\theta-\left(I_2+b^2m\right)\cdot\sin\theta-hbm\cdot(1+\cos\theta)+2hbm\cdot\cos^2\theta\right)\cdot\dot{\varphi}^2=\\&=-hm\cdot\ddot{u}_{gx}\cdot\cos\varphi\cdot\cos\theta-bm\cdot\ddot{u}_{gx}\cdot\cos\varphi\cdot\sin\theta-hm\cdot\ddot{u}_{gy}\cdot\sin\varphi\cdot\cos\theta-bm\cdot\ddot{u}_{gy}\sin\varphi\cdot\sin\theta\end{aligned}\tag{18}$$

$$\begin{gathered}\left(\left(I_1-I_2+h^2m-b^2m\right)\cdot\sin^2\theta+2\cdot\left(I_2+b^2m\right)\cdot\left(1-\cos\theta\right)+2hbm\cdot\sin\theta\cdot\left(1-\cos\theta\right)\right)\cdot\ddot{\varphi}+\\ \left(2\cdot\left(I_2-I_1-h^2m+b^2m\right)\cdot\sin\theta\cdot\left(1-\cos\theta\right)+2hbm\cdot\left(2\sin^2\theta+\cos\theta-1\right)+2\cdot\left(I_1+h^2m\right)\cdot\sin\theta\right)\cdot\dot{\varphi}\cdot\dot{\theta}=\\ =-bm\cdot\ddot{u}_{gy}\cdot\left(1-\cos\theta\right)\cos\varphi+bm\cdot\ddot{u}_{gx}\cdot\sin\varphi\cdot\left(1-\cos\theta\right)-hm\cdot\ddot{u}_{gy}\cdot\sin\theta\cos\varphi+hm\cdot\ddot{u}_{gx}\cdot\sin\varphi\cdot\sin\theta\end{gathered} \tag{19}$$

where I_1 is I_x and I_2 is I_z. Using Eq. (16) and defining

$$R=\sqrt{h^2+b^2} \tag{20}$$

Eq. (18) and (19) become:

$$\begin{aligned}\ddot{\theta}=&-p^2\left(\sin\left(\alpha-\theta\right)+\cos\left(\alpha-\theta\right)\left(\cos\varphi\cdot\frac{\ddot{u}_{gx}}{g}+\sin\varphi\cdot\frac{\ddot{u}_{gy}}{g}\right)\right)\\ &-\begin{pmatrix}\left(\frac{5}{4}\sin^2\alpha-\frac{4}{3}\cos^2\alpha\right)\cdot\cos\theta\cdot\sin\theta-\frac{3}{2}\sin^2\alpha\cdot\sin\theta-\\ -\cos\alpha\cdot\sin\alpha\cdot\left(1+\cos\theta\right)+2\cos\alpha\cdot\sin\alpha\cdot\cos^2\theta\end{pmatrix}\cdot\frac{1}{\left(\frac{5}{4}+\frac{1}{12}\cos^2\alpha\right)}\dot{\varphi}^2\end{aligned} \tag{21}$$

$$\begin{gathered}\left(\frac{1}{12}\left(3-18\sin^2\alpha+13\cos^2a\right)\cdot\sin^2\theta+3\left(1-\cos\theta\right)+2\sin\alpha\cos\alpha\sin\theta\cdot\left(1-\cos\theta\right)\right)R\cdot\ddot{\varphi}+\\ \left(3\sin^2\alpha\sin\theta+\frac{1}{6}\left(3-18\sin^2\alpha+13\cos^2\alpha\right)\sin\theta\cos\theta+2\cos\alpha\sin\alpha\left(2\sin^2\theta+\cos\theta-1\right)\right)R\cdot\dot{\varphi}\cdot\dot{\theta}=\\ =\left(\sin\alpha-\sin\left(\theta-\alpha\right)\right)\left(\ddot{u}_{gx}\sin\varphi-\ddot{u}_{gy}\cos\varphi\right)\end{gathered} \tag{22}$$

where p is the well-known frequency parameter from the response analysis of the 2d rocking block:

$$p^2=\frac{mgR}{I_o}=\frac{12}{15+\cos^2\alpha}\frac{g}{R} \tag{23}$$

where I_o is the moment of inertia of the cylinder around a point on the circumference of its base. By setting $\dot{\varphi}=0$ in Eq. (21) and using single-horizontal-component ground excitation one recovers the equation of the 2d rocking motion of a cylinder. However, unlike the equations used to describe the 2d rocking problem (which are non-smooth as they have to treat impact) the equations presented herein are smooth: θ is always positive and the change of contact point is a continuous function of φ. There is no instantaneous impact, but the numerical results presented in a next section sometimes show a very rapid (but continuous) change of the pivot point.

Due to the above, for the equations of motion to be solved numerically, 3d motion has to be excited: in the case of free vibration via a non-zero initial spin, $\dot{\varphi}$, and in the case of earthquake excitation via applying a two-horizontal-component ground excitation.

Using Eq. (21) and by assuming a constant cylinder tilt angle θ and no ground excitation one can get the period of cylinder wobbling as a function of θ.

$$T=\frac{2\pi}{p}\sqrt{-\frac{\begin{pmatrix}\left(\frac{5}{4}\sin^2\alpha-\frac{4}{3}\cos^2\alpha\right)\cdot\cos\theta\cdot\sin\theta-\frac{3}{2}\sin^2\alpha\cdot\sin\theta-\\ -\cos\alpha\cdot\sin\alpha\cdot\left(1+\cos\theta\right)+2\cos\alpha\cdot\sin\alpha\cdot\cos^2\theta\end{pmatrix}}{\sin\left(\alpha-\theta\right)\left(\frac{5}{4}+\frac{1}{12}\cos^2\alpha\right)}} \tag{24}$$

Fig. 3 plots Eq. (24) for different values of cylinder slenderness tanα. The $\tan\alpha$=1000 value corresponds to a spinning disk. The figure also plots the period of a 2d rocking block, as derived by Housner [3]. Note that

Housner's derivation is linearized and holds only for small values of α (and then it is independent of the exact value of α).

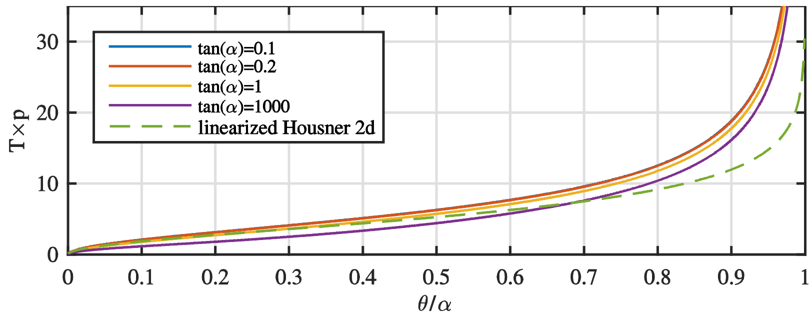

Fig. 3 Period – Tilt angle dependence of the cylinder wobbling period.

2.3 Uplift condition

Uplift occurs when the total ground acceleration is larger than gtanα:

$$\sqrt{\ddot{u}_{gx}^2 + \ddot{u}_{gy}^2} \geq g \tan\alpha \tag{25}$$

The uplift occurs towards the direction of the D'Alembert inertia forces at the instant of uplift. This direction is given by the angle φ_0

$$\cos\varphi_0 = -\frac{u_{gx}}{\sqrt{\ddot{u}_{gx}^2 + \ddot{u}_{gy}^2}} \quad \text{and} \quad \sin\varphi_0 = -\frac{u_{gy}}{\sqrt{\ddot{u}_{gx}^2 + \ddot{u}_{gy}^2}} \tag{26}$$

3 Free vibration results

The above equations are implemented in Matlab and solved numerically. Fig. 4 plots three characteristic R=6m and tanα=0.2 rigid cylinder rocking and wobbling modes in free vibration from a given initial condition. For a very small initial spin (Fig.4 a,b), the cylinder changes its pivot point rapidly (but smoothly, as the solution is continuous). The change of pivot point is defined by an angle of turn, slightly larger than π, which compares well with the prediction of [53]. The abrupt change of pivot point generates large vertical forces at the contact point (in the limit case they become infinite and the motion tends to an impact). Therefore, one source of damping of a wobbling cylinder can be such impact mechanism. However, this model cannot account for such energy dissipation.

Fig.4 (c,d) plots the results for an initial spin defined through Eq. (24). The tilt angle stays constant and the cylinder only wobbles without rocking. Fig. 4 (e.f) plots a combination of the above two modes of vibration.

4 Ground motion results

The cylinder with R=6m and tanα=0.2 is excited by the 1940 El Centro ground motion (shown in the bottom two rows of Fig. 5). The x-direction excitation is the EW component and the y-direction excitation is the NS component of this motion. The results show that angle φ changes abruptly during the more intense part of the ground motion. Contrary, when the ground motion becomes weaker, the cylinder follows a quasi-free vibration motion and the movement of the contact point is slower and smoother.

5 Overturning Spectra

In order to gain insight into the stability of rigid cylinders of different sizes, so called "rocking spectra" are constructed by scaling El Centro ground motion. The authors acknowledge that such a scaling is not realistic. However, it is performed as a first approach to the problem. Fig. 6 (a-c) plots these overturning spectra (i.e.

contour plots of maximum tilt angle, θ) and minimum overturning acceleration spectra (Fig. 6 d), for a given cylinder slenderness tanα=0.1. The abscissa defines the size of the cylinder (through its semidiagonal, R). The ordinate defines the normalized maximum acceleration of the total two–horizontal-component ground excitation and of the EW and NS component. Fig. 6(a) shows the 3d response to the scaled El Centro ground motion while Fig. 6 (b) and Fig. 6 (c) plot the 2d response to the two components of the same ground motion. In order to make the results comparable, no damping has been included in the planar models. One can observe that for large blocks, planar analysis is unconservative.

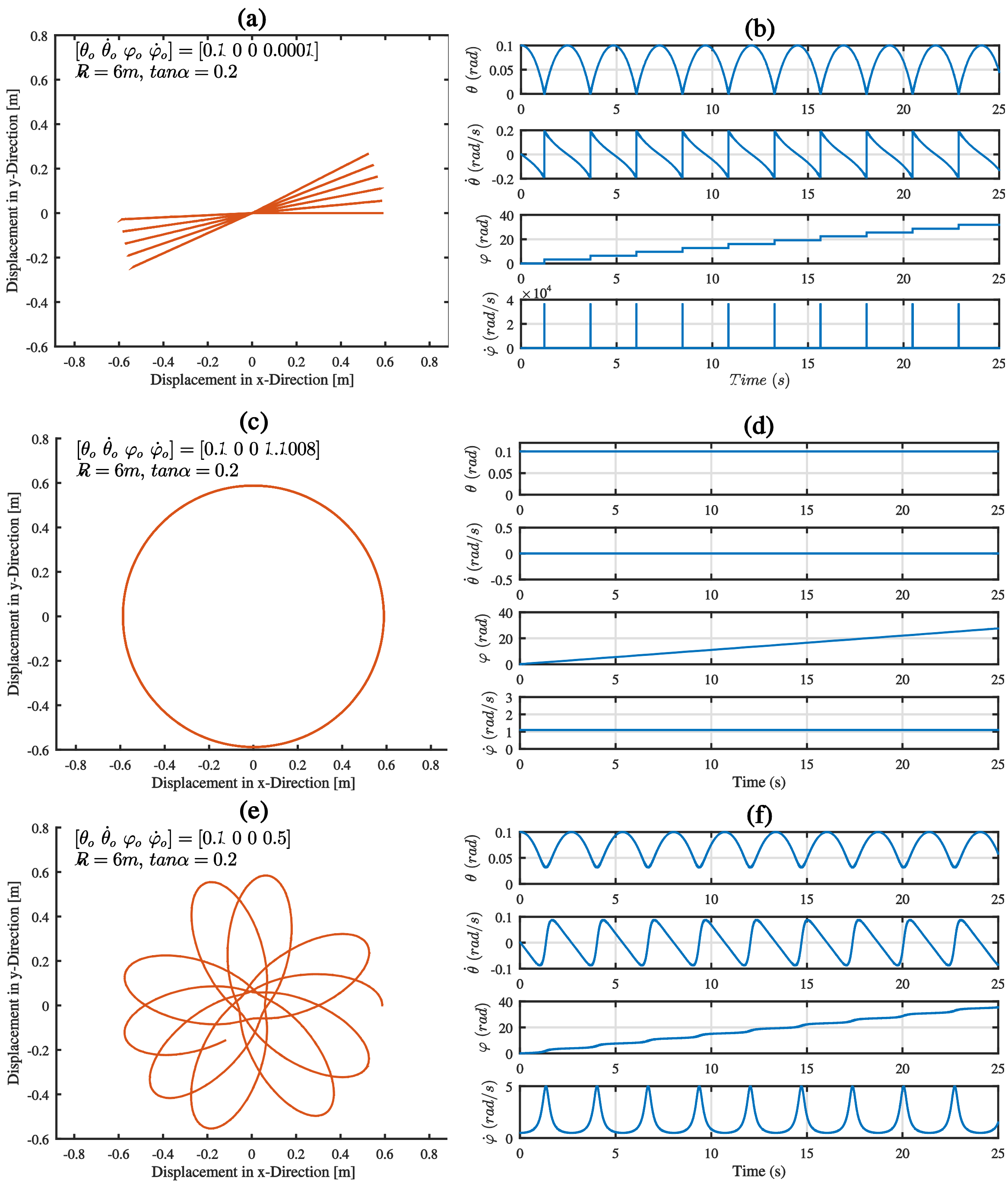

Fig. 4 Orbits of the center of mass (left) and $\theta, \dot{\theta}$, φ and $\dot{\varphi}$ time histories for free vibration with different initial conditions (right).

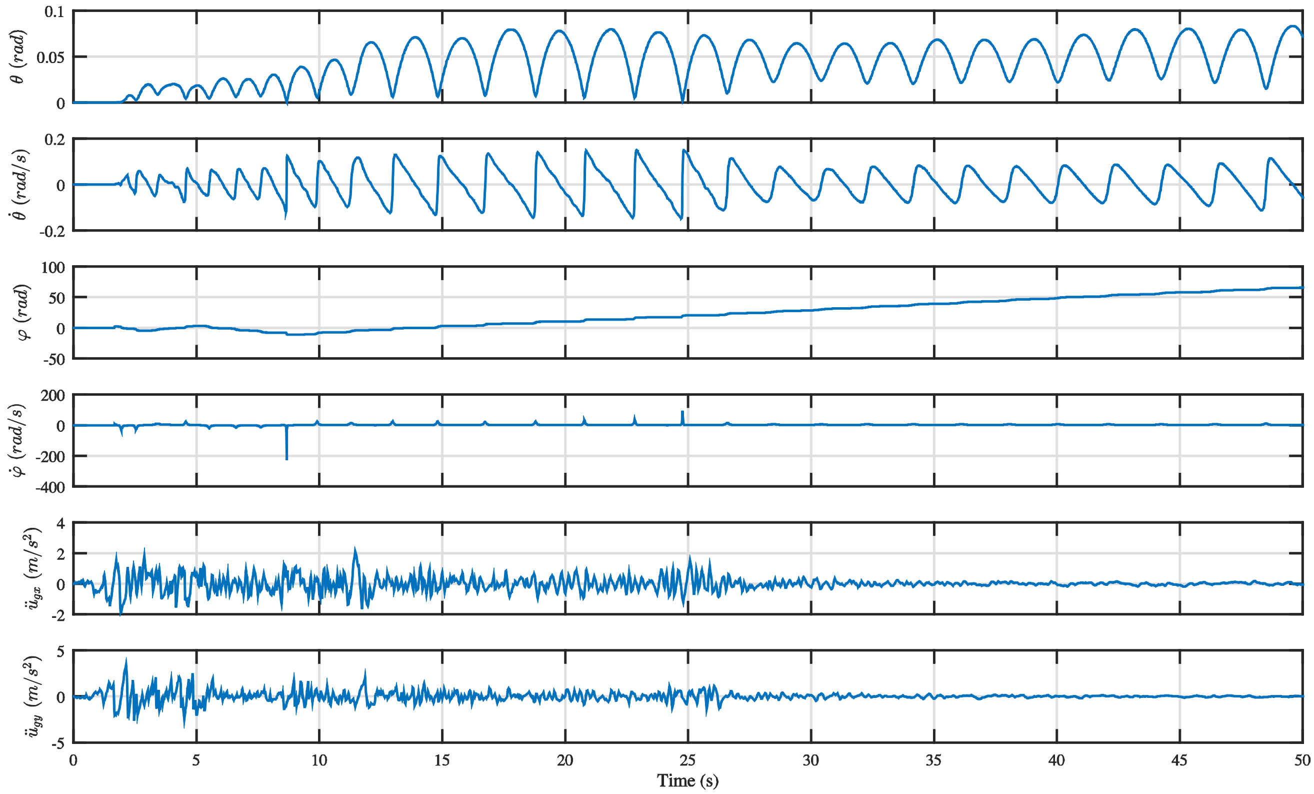

Fig. 5 $\theta, \dot{\theta}$, φ and $\dot{\varphi}$ time histories (top 3 rows) for the 1940 El Centro ground motion (bottom 2 rows).

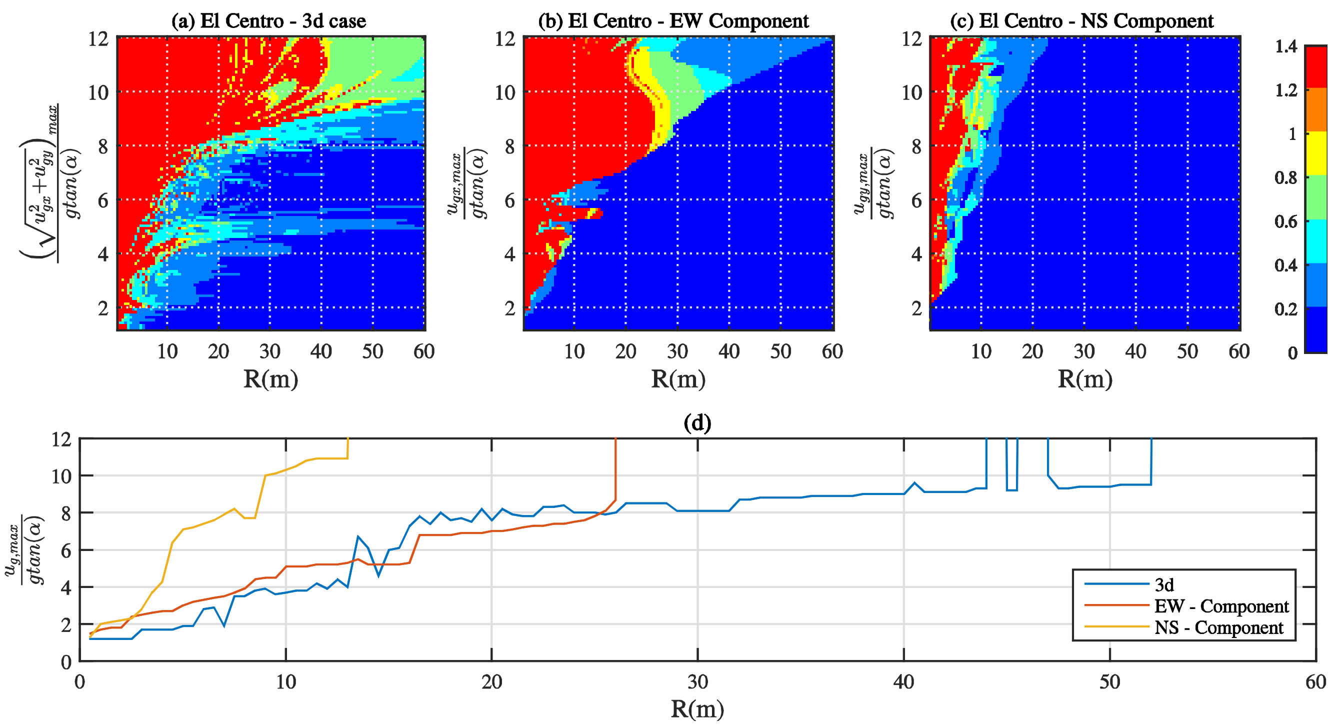

Fig. 6. *Top*: θ/α Contour plots for different column sizes, *R*, and for scaled 1940 El Centro ground motion *Bottom:* Minimum overturning acceleration spectra of the top plots.

6. Conclusions

A two-degree-of-freedom model that describes the 3d rocking and wobbling (unsteady rolling) motion of a rigid cylinder was developed. The model describes the dynamic behavior of rigid cylindrical columns that can uplift, rock and wobble with the constraint that they do not slide or roll-out of their original position. This assumption is adequate to describe cylinders whose roll-out motion is prevented e.g. through a recess. The model is the simplest 3d extension of the 2d Housner rigid body rocking model. It was used to study the response of a rigid cylinder in free vibration as well as under earthquake ground motion excitation. The out of plane motion was intense and changed the nature of the cylinder response. For the 1940 ElCentro ground motion, it was found that the 2d model generally gives unconservative estimates of the overturning ground motion intensity.

7. References

[1] Milne J (1885): Seismic experiments, *Trans. Seismol. Soc. Jpn*. **8**, 1–82.

[2] Kirkpatrick P (1927): Seismic measurements by the overthrow of columns, *Bull. Seismol. Soc. Am*. **17**, 95–109.

[3] Housner, GW (1963): The behaviour of inverted pendulum structures during earthquakes, *Bull. Seismol. Soc. Am.* **53**, 404–417.

[4] Yim CS, Chopra AK, and Penzien J (1980): Rocking response of rigid blocks to earthquakes, *Earthq. Eng. Struct. Dyn*., (**8)** 565–587.

[5] Psycharis IN and Jennings PC (1983): Rocking of slender rigid bodies allowed to uplift, Earthq. Eng. Struct. Dyn., **11** (1), 57–76.

[6] Makris N and Roussos Y (1998): Rocking response and overturning of equipment under horizontal pulse-type motion, Rept. No. PEER Report-98/05.

[7] Zhang J and Makris N (2001): Rocking Response of Free-Standing Blocks under Cycloidal Pulses, *J. Eng. Mech*., **127** (5), 473–483.

[8] Makris N and Konstantinidis D (2003): The rocking spectrum and the limitations of practical design methodologies, *Earthq. Eng. Struct. Dyn*., **32** (2), 265–289.

[9] Oliveto G, Caliò I, and Greco A (2003): Large displacement behaviour of a structural model with foundation uplift under impulsive and earthquake excitations, *Earthq. Eng. Struct. Dyn*., **32** (3), 369–393.

[10] Peña F, Prieto F, Lourenço PB, Campos Costa A, and Lemos JV (2007): On the dynamics of rocking motion of single rigid-block structures, *Earthq. Eng. Struct. Dyn*., **36** (15), 2383–2399.

[11] Contento A and Di Egidio A (2009): Investigations into the benefits of base isolation for non-symmetric rigid blocks, *Earthq. Eng. Struct. Dyn*., **38** (7), 849–866.

[12] Konstantinidis D and Makris N (2009): Experimental and analytical studies on the response of freestanding laboratory equipment to earthquake shaking, *Earthq. Eng. Struct. Dyn*., **38** (6), 827–848.

[13] Konstantinidis D and Makris N (2010): Experimental and analytical studies on the response of 1/4-scale models of freestanding laboratory equipment subjected to strong earthquake shaking, *Bull. Earthq. Eng*., **8** (6), 1457–1477.

[14] Ma QTM, (2010): The mechanics of rocking structures subjected to ground motion (PhD Dissertation, University of Auckland, NZ.)

[15] ElGawady Ma, Ma QTM, Butterworth JW, and Ingham J (2011): Effects of interface material on the performance of free rocking blocks, *Earthq. Eng. Struct. Dyn*., **40** (4), 375–392.

[16] Acikgoz S and DeJong MJ (2012): The interaction of elasticity and rocking in flexible structures allowed to uplift, *Earthq. Eng. Struct. Dyn*., **41** (11), 1–18.

[17] Dimitrakopoulos EG and DeJong MJ (2012): Revisiting the rocking block: closed-form solutions and similarity laws, *Proc. R. Soc. A Math. Phys. Eng. Sci*., **468** (2144), 2294–2318.

[18] Dimitrakopoulos EG and DeJong MJ (2012): Overturning of Retrofitted Rocking Structures under Pulse-Type Excitations, *J. Eng. Mech*., **138** (8), 963–972.

[19] Vassiliou MF and Makris N (2012): Analysis of the rocking response of rigid blocks standing free on a seismically isolated base, *Earthq. Eng. Struct. Dyn*., **41** (2), 177–196.

[20] Dimitrakopoulos EG and De Jong MJ (2013), Seismic overturning of rocking structures with external viscous dampers, *Computational methods in earthquake engineering*, Springer.

[21] Vassiliou MF, Mackie KR, and Stojadinović B (2013): Rocking Response of Slender, Flexible Columns under Pulse Excitation, *Proceedings of the 4th ECCOMAS Thematic Conference on Computational Methods in Structural Dynamics and Earthquake Engineering*, Kos Island, Greece.

[22] Acikgoz S and DeJong MJ (2014): The rocking response of large flexible structures to earthquakes, *Bull. Earthq. Eng.*, ***12** (2)*, 875–908.

[23] DeJong MJ and Dimitrakopoulos EG (2014): Dynamically equivalent rocking structures, *Earthq. Eng. Struct. Dyn.,* **43** (10), 1543–1563.

[24] Makris N, The Role of the Rotational Inertia on the Seismic Resistance of Free-Standing Rocking Columns and Articulated Frames (2014): *Bull. Seismol. Soc. Am*., **104** (5), 2226–2239.

[25] Dimitrakopoulos EG and Paraskeva TS (2015): Dimensionless fragility curves for rocking response to near-fault excitations, *Earthq. Eng. Struct. Dyn*., **44** (12), 2015–2033.

[26] Makris N, A half-century of rocking isolation (2014): Earthquakes Struct., **7** (6), 1187–1221.

[27] Truniger RE, Vassiliou MF, and Stojadinović B (2015): An analytical model of a deformable cantilever structure rocking on a rigid surface: experimental validation, *Earthq. Eng. Struct. Dyn*., **44** (13).

[28] Vassiliou MF and Makris N (2015): Dynamics of the Vertically Restrained Rocking Column, *J. Eng. Mech*., 141 (12), p. 04015049.

[29] Vassiliou MF, Truniger RE, and Stojadinović B (2015): An analytical model of a deformable cantilever structure rocking on a rigid surface: development and verification, *Earthq. Eng. Struct. Dyn*., **44** (13).

[30] Makris N and Kampas G (2016): Size Versus Slenderness: Two Competing Parameters in the Seismic Stability of Free-Standing Rocking Columns, *Bull. Seismol. Soc. Am*., **106** (1), 104–122.

[31] Bakhtiary E and Gardoni (2016): P, Probabilistic seismic demand model and fragility estimates for rocking symmetric blocks, *Eng. Struct.*, **114**, 25–34.

[32] Bachmann JA, Blöchlinger P, Wellauer M, Vassiliou MF, and Stojadinović B (2016): Experimental investigation of the seismic response of a column rocking and rolling on a concave base ECCOMAS Congress 2016: 7th European Congress on Computational Methods in Applied Sciences and Engineering, 2016.

[33] Makris N and M. F. Vassiliou MF (2012): Sizing the slenderness of free-standing rocking columns to withstand earthquake shaking, *Arch. Appl. Mech*., **82** (10–11), 1497–1511.

[34] Konstantinidis D and Makris N (2005): Seismic response analysis of multidrum classical columns, *Earthq. Eng. Struct. Dyn*. **34** (10), 1243–1270.

[35] Papaloizou L and Komodromos P (2009): Planar investigation of the seismic response of ancient columns and colonnades with epistyles using a custom-made software, *Soil Dyn. Earthq. Eng.*, **29** (11–12), 1437–1454.

[36] Makris N. and Vassiliou MF (2013): Planar rocking response and stability analysis of an array of free-standing columns capped with a freely supported rigid beam," *Earthq. Eng. Struct. Dyn*., **42** (3) 431–449.

[37] Drosos V and Anastasopoulos I (2014): Shaking table testing of multidrum columns and portals, *Earthq. Eng. Struct. Dyn.*, **43** (11), 1703–1723.

[38] Makris N and Vassiliou MF (2014): Are Some Top-Heavy Structures More Stable? *J. Struct. Eng*., **140** (5), p. 06014001.

[39] Makris N and Vassiliou MF (2015): Dynamics of the Rocking Frame with Vertical Restrainers, *J. Struct. Eng*., **141** (10), p. 04014245.

[40] Dimitrakopoulos EG and Giouvanidis AI (2015): Seismic Response Analysis of the Planar Rocking Frame, *J. Eng. Mech.*, **141** (7), p. 04015003.

[41] Makris N and Vassiliou MF (2015): The dynamics of the rocking frame, in Seismic Assessment, *Behavior and Retrofit of Heritage Buildings and Monuments*, Springer, 37–59.

[42] Makris N and Vassiliou MF (2015): Seismic Response and Stability of the Rocking Frame, *Computational Methods, Seismic Protection, Hybrid Testing and Resilience in Earthquake Engineering*, Springer, 249–273.

[43] Koh AS and Mustafa G (1990): Free rocking of cylindrical structures. *Journal of engineering mechanics*, **116**(1), 35-54.

[44] Koh AS and Hsiung CM (1991): Base isolation benefits of 3-D rocking and uplift. I: Theory. *Journal of engineering mechanics*, **117**(1), 1-18.

[45] Koh AS and Hsiung CM (1991): Base isolation benefits of 3-D rocking and uplift. II: Numerical Example. *Journal of engineering mechanics*, **117**(1), 19-31.

[46] Ambraseys, N., & Psycharis, I. N. (2011). Earthquake stability of columns and statues. *Journal of Earthquake Engineering*, **15**(5), 685-710.

[47] Stefanou I, Psycharis I, & Georgopoulos IO (2011). Dynamic response of reinforced masonry columns in classical monuments. *Construction and Building Materials*, **25**(12), 4325-4337.

[48] Krstevska, L., Mihailov, V., Boschi, E., & Rovelli, A. (1996). Experimental dynamic testing of prototype and model of the Antonina Column in Roma. *Proceedings of the 11th world conference on earthquake engineering*. Paper (No. 546).

[49] Mouzakis, H. P., Psycharis, I. N., Papastamatiou, D. Y., Carydis, P. G., Papantonopoulos, C., & Zambas, C. (2002). Experimental investigation of the earthquake response of a model of a marble classical column. *Earthquake engineering & structural dynamics*, **31**(9), 1681-1698.

[50] Drosos, V., & Anastasopoulos, I. (2014). Shaking table testing of multidrum columns and portals. *Earthquake Engineering & Structural Dynamics*, 43(11), 1703-1723.

[51] Makris N, Alexakis H, Kampas G, Strepelias I, Kolonas C and Bousias S (2015): *Seismic protection of bridges with rocking piers which recenter with gravity,* Report EEAM, 2015-01, University of Patras Department of Civil Engineering

[52] Stefanou, I., Vardoulakis, I., & Mavraganis, A. (2011). Dynamic motion of a conical frustum over a rough horizontal plane. *International Journal of Non-Linear Mechanics*, 46(1), 114-124.

[53] Srinivasan M and Ruina A. (2008); Rocking and rolling: a can that appears to rock might actually roll. *Physical Review E*, **78**(6), 066609.

[54] Moffatt HK (2000): Euler's disk and its finite-time singularity. *Nature*, **404**(6780), 833-834.

[55] van den Engh G, Nelson P, Roach J (2000). Numismatic gyrations. *Nature,* **408** (6812) 540.

[56] McDonald AJ, McDonald KT(2000). The rolling motion of a disk on a horizontal plane. Preprint Archive, Los Alamos National Laboratory. *arXiv: physics*/008227.

[57] Moffatt HK (2000): Reply to "Numismatic gyrations". *Nature* **408** (6812) 540.

[58] Kessler P and O'Reilly OM (2002): The ringing of Euler's disk. *Regular and Chaotic dynamics*, **7**(1), 49-60.

[59] Konstantinidis D and Makris N (2007): The dynamics of a rocking block in three dimensions, 8th Hell. Soc. Theor. Appl. Mech. Int. Congr. Mech. Patras, Greece September 2015.

[60] Zulli D, Contento A, and Di Egidio A (2102): 3D model of rigid block with a rectangular base subject to pulse-type excitation, *Int. J. Non. Linear. Mech*., **47** (6), 679–687.

[61] Chatzis, MN, and Smyth AW (2012). Modeling of the 3D rocking problem. *International Journal of Non-Linear Mechanics*, **47**(4) 85-98.

[62] Chatzis, M. N., & Smyth, A. W. (2012). Three-dimensional dynamics of a rigid body with wheels on a moving base. *Journal of Engineering Mechanics*, **139**(4), 496-511.

[63] Greenbaum, R. J., Smyth, A. W., & Chatzis, M. N. (2015). Monocular Computer Vision Method for the Experimental Study of Three-Dimensional Rocking Motion. *Journal of Engineering Mechanics*, **142**(1), 04015062.

[64] Ginsberg, J. H. (1998). *Advanced engineering dynamics*. Cambridge University Press.